NASA TECHNICAL NOTE

NASA TN D-6447

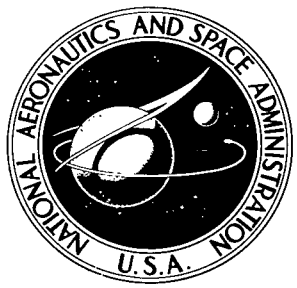

SENSOR FOR DETECTING METEOROID PENETRATION OF PRESSURIZED CELLS

by Leonard R. McMaster

Langley Research Center
Hampton, Va. 23365

NATIONAL AERONAUTICS AND SPACE ADMINISTRATION • WASHINGTON, D. C. • SEPTEMBER 1971

1. Report No.	2. Government Accession No.	3. Recipient's Catalog No.
NASA TN D-6447		

4. Title and Subtitle

SENSOR FOR DETECTING METEOROID PENETRATION OF PRESSURIZED CELLS

5. Report Date: September 1971

6. Performing Organization Code:

7. Author(s)

Leonard R. McMaster

8. Performing Organization Report No.: L-7794

9. Performing Organization Name and Address

NASA Langley Research Center
Hampton, Va. 23365

10. Work Unit No.: 746-03-47-02

11. Contract or Grant No.:

12. Sponsoring Agency Name and Address

National Aeronautics and Space Administration
Washington, D.C. 20546

13. Type of Report and Period Covered: Technical Note

14. Sponsoring Agency Code:

15. Supplementary Notes

16. Abstract

An experimental investigation was made to determine the feasibility of using a cold-cathode glow discharge tube to detect the meteoroid puncture of pressurized cells. By using various electrode configurations, electrode materials and ionizing gas compositions, several glow discharge tubes were constructed and tested to determine a combination that would give operational characteristics suitable for this purpose.

It was demonstrated that this device would operate like a switch, conducting current only when a particular pressure range was reached during the depressurization of a punctured cell. In addition, the time rate of change of current during a discharge was found to vary proportionally with the leak rate, and thereby puncture size could be determined. Particularly advantageous is the more than 80 times reduction in weight of this sensor compared with the presently used diaphragm-actuated microswitch.

17. Key Words (Suggested by Author(s))	18. Distribution Statement
Glow discharge tube Meteoroid detector	Unclassified – Unlimited

19. Security Classif. (of this report)	20. Security Classif. (of this page)	21. No. of Pages	22. Price*
Unclassified	Unclassified	30	$3.00

*For sale by the National Technical Information Service, Springfield, Virginia 22151

SENSOR FOR DETECTING METEOROID PENETRATION OF PRESSURIZED CELLS

By Leonard R. McMaster
Langley Research Center

SUMMARY

An experimental investigation was made to determine the feasibility of using a cold-cathode glow discharge tube to detect the meteoroid puncture of pressurized cells. By using various electrode configurations, electrode materials, and ionizing gas compositions, several glow discharge tubes were constructed and tested to determine a combination that would give operational characteristics suitable for this purpose.

It was demonstrated that this device would operate like a switch, conducting current only when a particular pressure range was reached during the depressurization of a punctured cell. In addition, the time rate of change of current during a discharge was found to vary proportionally with the leak rate, and thereby puncture size could be determined. Particularly advantageous is the more than 80 times reduction in weight of this sensor compared with the presently used diaphragm-actuated microswitch.

INTRODUCTION

The possible danger in an encounter between meteoroids and a spacecraft has resulted in various research activities designed to define the meteoroid environment in space and its effect on spacecraft. The most straightforward way of determining meteoroid hazards to spacecraft is by penetration techniques. One such technique employs a simple one-shot device referred to as a pressurized cell detector. It consists of a gas-pressurized cell equipped with a pressure sensor. When a meteoroid punctures the cell, the gas leaks out, and the loss of pressure is detected by the pressure sensor (ref. 1).

The pressure sensor presently used with pressurized cell detectors is a diaphragm-actuated microswitch. To date, no attempt has been made to determine the size of a puncture by use of these sensors, even though a method exists as follows: Two switches are installed and set to actuate at different pressures, the time interval between their actuations giving the leak rate and, thereby, the size of the hole. The mass (78 g) and volume (34 cm^3) of these mechanical switches make their use in large quantities prohibitive, and if penetration size is to be obtained, as well as a record of the event, their use is even more undesirable because the mass and volume are doubled. (These switches are to be

part of the meteoroid detector bumper on the Meteoroid Technology Satellite scheduled for launch during the first quarter of 1972.)

A review of the proposed investigation of the meteoroid population through interplanetary space, by use of pressurized cell detectors, indicated a need for a pressure sensor considerably reduced in mass (0.9 g) and volume from those currently used. This paper discusses the development of such a pressure sensor, which can be described as a simple cold-cathode glow discharge tube operating with an electric potential V_a applied across two electrodes that are mounted inside the gas-pressurized cell (fig. 1). The

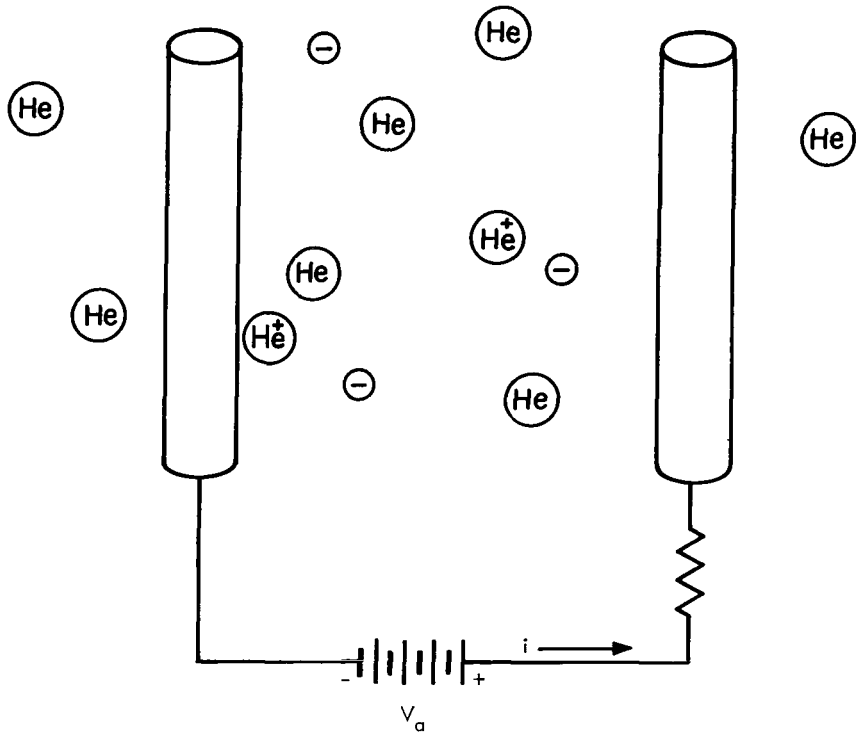

Figure 1.- Diagram of a cold-cathode glow discharge tube.

applied potential is insufficient to cause a breakdown between the electrodes at the initial molecular density within the cell. However, when a cell is punctured in the vacuum of space, gas flow will occur across the pressure differential, and the density will decrease to a value where a discharge, similar to that of a neon glow lamp, will occur. The glow discharge tube operates like a pressure switch, indicating an open circuit before a puncture and indicating a closed circuit, by allowing a current to flow between the electrodes, after a puncture. As the gas density within the detector cell continues to decrease after a breakdown, the current flow between the electrodes also decreases until it can no longer be maintained. Recording the current flow through the discharge tube then gives a history of the events resulting from the puncture of the detector cell, that is, a record of the gas leak rate; hence, the size of the puncture can be determined.

SYMBOLS

A	orifice area, m^2
a,b	constants, A
a_o	constant, m^2
a_1	constant, m^2-sec/A
d	electrode separation, m
E	electrostatic field, V/m
f	function of i or p_o
i	discharge current, A
i_o	primary current, A
K	constant, m/sec
k	Boltzmann constant
M	mass of gas molecule, kg
N	number of molecules in a given volume
N_o	number of primary electrons leaving the cathode per second
P	breakdown probability
p	pressure, N/m^2
p_i	initial pressure, N/m^2
p_o	reduced gas pressure (0^o C), N/m^2
p_1	pressure upstream from orifice, N/m^2
p_2	pressure downstream from orifice, N/m^2
Q	flow rate, J/sec
q	average number of secondary electrons leaving the cathode per primary electron emitted

R_1	current-limiting resistance, ohms
R_2	output-signal resistance, ohms
r	ratio of downstream to upstream pressure
T	temperature, ^{o}K
t	time, sec
t_s	statistical time lag, sec
V	volume, m^3
V_a	applied voltage, V
V_i	ionization potential, V
V_r	running voltage, V
V_s	breakdown voltage, V
γ	number of electrons released per positive ion collision with the cathode; ratio of specific heats of a gas
η_i	number of ion pairs created by an electron in moving through a potential difference of 1 volt
θ,Φ	functions of E and p_o
ψ	function of p_o and d

Subscripts:

max	maximum
min	minimum

THEORY

Breakdown Phenomenon

To completely understand the phenomenon of breakdown and current flow in a gas, it is necessary to study the fundamental principles of the motions of electrons and ions in gases, the statistical equilibrium of such combinations, and the various ionization processes that can occur in the gas or at the electrode surfaces. These subjects, however,

will not be discussed in this paper, as they are adequately covered in previous literature (refs. 2, 3, and 4). The mathematical formulation of the breakdown mechanism will only be introduced to show its dependence on certain parameters.

A gas in its normal state is almost a perfect insulator, but when an electric field of sufficient intensity is created in a gas between two electrodes, the gas can become a conductor. This transition from an insulating to a conducting state is called the electrical breakdown. However, before breakdown can occur in a previously insulating gas, the initial current – possibly consisting of only a few initiatory electrons – must be increased by some ionization mechanism. To illustrate how this occurs, figure 2 shows

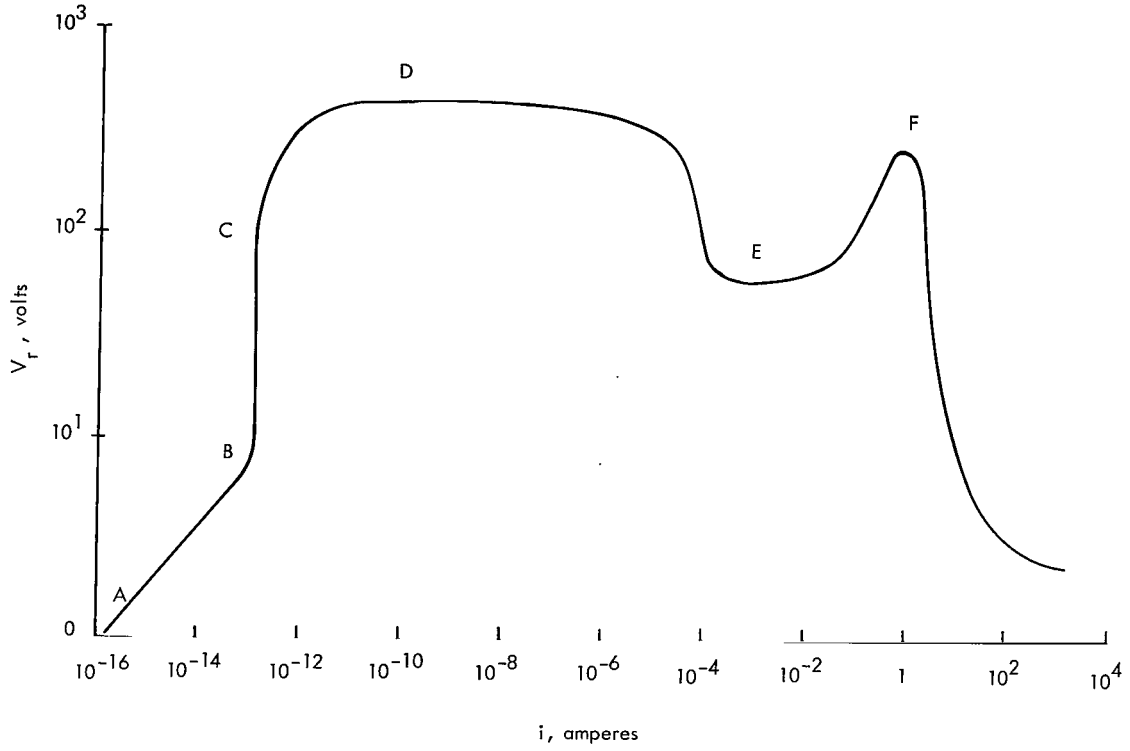

Figure 2.- Schematic characteristic $V_r = f(i)$ of a gas discharge between flat parallel plates.

the relationship between the discharge current and the voltage drop across a discharge tube with flat, parallel plates and constant gas density and temperature. Initially (point A in fig. 2), a state of partial ionization exists in a discharge tube even in the absence of light and radioactive additives. This ionization, resulting in a primary current i_o, is due to external agents such as cosmic rays and is subject to statistical fluctuations. The current increases from point A to point B as more and more of the ionized gas particles are drawn to the cathode by the increasing electric field. The constant-current region from point B to point C indicates that all available ionized particles are being collected.

Beyond point C the electric field accelerates the gas ions sufficiently to produce secondary ions in such a manner that increasing the voltage results in the current increasing exponentially. This increasing current, caused by ion multiplication, leads to a non-self-maintained, or Townsend discharge at point D. Increasing the voltage even further causes the discharge tube to "breakdown," and the current will continue to increase to a value limited primarily by the resistance of the external circuitry. The region surrounding point E is referred to as glow discharge, and the high-current region beyond point F is known as arc discharge.

The total ionization current in a discharge tube can be approximated by the equation (ref. 2, p. 143)

$$i = \frac{i_o \exp \int_{V_i}^{V_a} \eta_i dV_a}{1 - \gamma\left[\exp\left(\int_{V_i}^{V_a} \eta_i dV_a\right) - 1\right]} \tag{1}$$

where the ionization coefficient η_i and the secondary emission coefficient γ are both functions of field strength and gas density. At breakdown the discharge current increases several orders of magnitude and thereby indicates that the denominator of equation (1) must approach zero. The condition for breakdown where $V_a = V_s$ is therefore

$$\gamma\left[\exp\left(\int_{V_i}^{V_s} \eta_i dV_a\right) - 1\right] = 1 \tag{2}$$

or

$$\int_{V_i}^{V_s} \eta_i dV_a = \ln\left(1 + \frac{1}{\gamma}\right) \tag{3}$$

Since

$$\eta_i = \Phi\left(\frac{E}{p_o}\right)$$

and

$$\gamma = \theta\left(\frac{E}{p_o}\right)$$

equation (3) can be written as

$$\int_{V_i}^{V_s} \Phi\left(\frac{E}{p_o}\right) dV_a = \ln\left[1 + \frac{1}{\theta\left(\frac{E}{p_o}\right)}\right] \tag{4}$$

Hence, for a given gas composition, electrode material, and electrostatic field strength, the voltage at which breakdown occurs V_S is only a function of the reduced gas pressure $V_S = f(p_o)$. (It should be noted that the dependence of V_S on the electrode material will be noticeable only if the electrode material is clean and degassed.) If allowance is made for variation in field strength, it is found that V_S depends on the product of the reduced gas pressure and some characteristic dimension of the electrode geometry, for example, $V_S = \psi(p_o d)$ for a parallel-plane electrode system with $E = V_S/d$ at breakdown. In this relationship, known as Paschen's law, the breakdown voltage exhibits a minimum at some medium pressure, as shown in figure 3. At both higher and lower

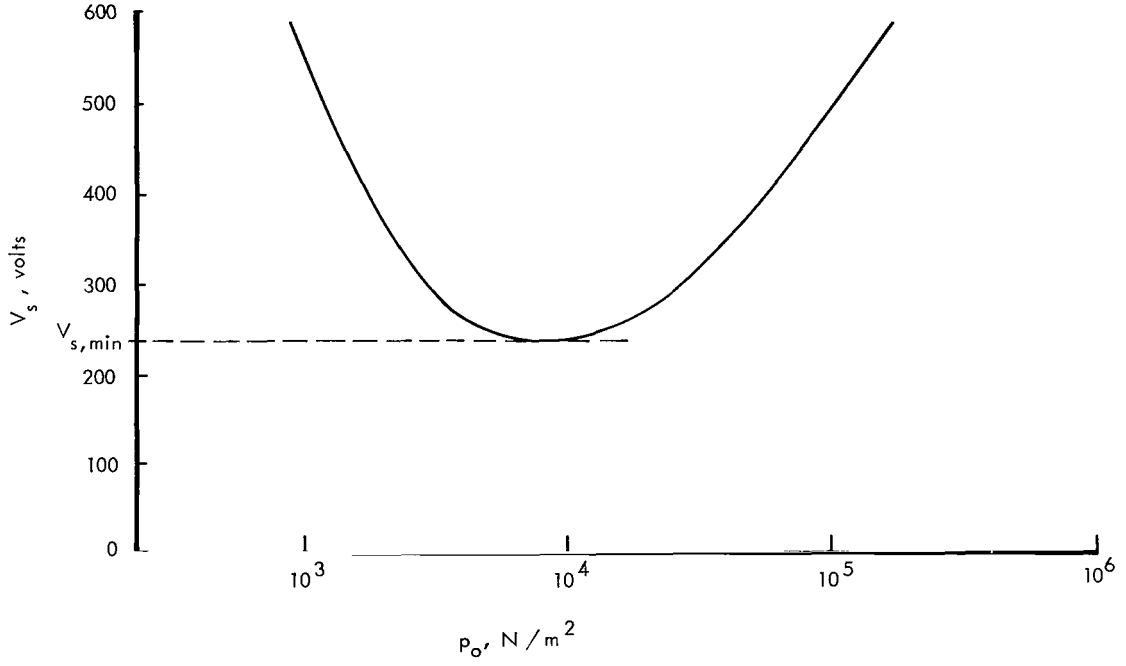

Figure 3.- Breakdown voltage V_S as a function of reduced gas pressure p_o.

pressures, relatively large voltages are required for breakdown. Without the increased electric field, the mean free path of the gas particles is too short at the higher pressures for them to gain enough energy for ionization between successive collisions. At the lower pressures the mean free path is so long that the probability of any collision is very small.

Since a glow discharge tube has the ability of returning to its insulating state after breakdown, it behaves, in essence, like a switch. When used with a pressurized cell to detect a puncture, it can be set up as an "ON-OFF" switch, with a loss of signal indicating a drop in pressure below some preset level in the conducting region (ref. 5), or as an "OFF-ON-OFF" switch, recording the signal produced as the pressure drops through the conducting region. The latter technique can also be used to measure the rate of pressure change through the conducting region, with the advantage of not drawing appreciable

current either before or a finite time after breakdown. This technique, therefore, was emphasized in this investigation.

Breakdown Probability

Even when the voltage applied to a discharge tube exceeds the voltage required for breakdown, a finite time elapses before the primary current can increase to a self-maintained discharge. This time lag consists of two parts, a statistical time lag and a formative time lag. The statistical time lag t_s is the time necessary for the appearance of a suitable initiatory electron, which will become sufficiently multiplied by ionization for breakdown to occur. The formative time lag is the time necessary for the various ionization processes to generate a self-maintained discharge from this initiatory electron. (See ref. 2, p. 129.) The statistical time lag, therefore, depends on the probability P that any particular electron leads to a breakdown and the number of primary electrons N_o leaving the cathode per second,

$$t_s = \frac{1}{PN_o} \tag{5}$$

However, to relate the breakdown probability to the voltage applied to the discharge tube, it is easier to define P in terms of the number of secondary electrons q being emitted from the cathode for each primary electron emitted,

$$P = 1 - \frac{1}{q} \tag{6}$$

where

$$q = \gamma\left[\exp\left(\int_{V_i}^{V_a} \eta_i dV_a\right) - 1\right] \tag{7}$$

From the breakdown condition given by equation (3), $q = 1$ for $V_a = V_s$, and the probability that a particular electron will cause breakdown approaches zero; that is, the statistical time lag for a suitable electron to appear is very long. To reduce the statistical time lag and allow $P \to 1$, an overvoltage $\Delta V = V_a - V_s$ must be applied to a discharge tube; for example, the overvoltage for a parallel plate geometry should be greater than $0.25V_s$ (ref. 2, pp. 132-133).

LABORATORY SETUP

In order to determine the optimum cold-cathode discharge tube to detect meteoroid punctures, a system was designed to evaluate several different experimental models. This system (fig. 4) consisted of a small vacuum chamber, with an internal volume of

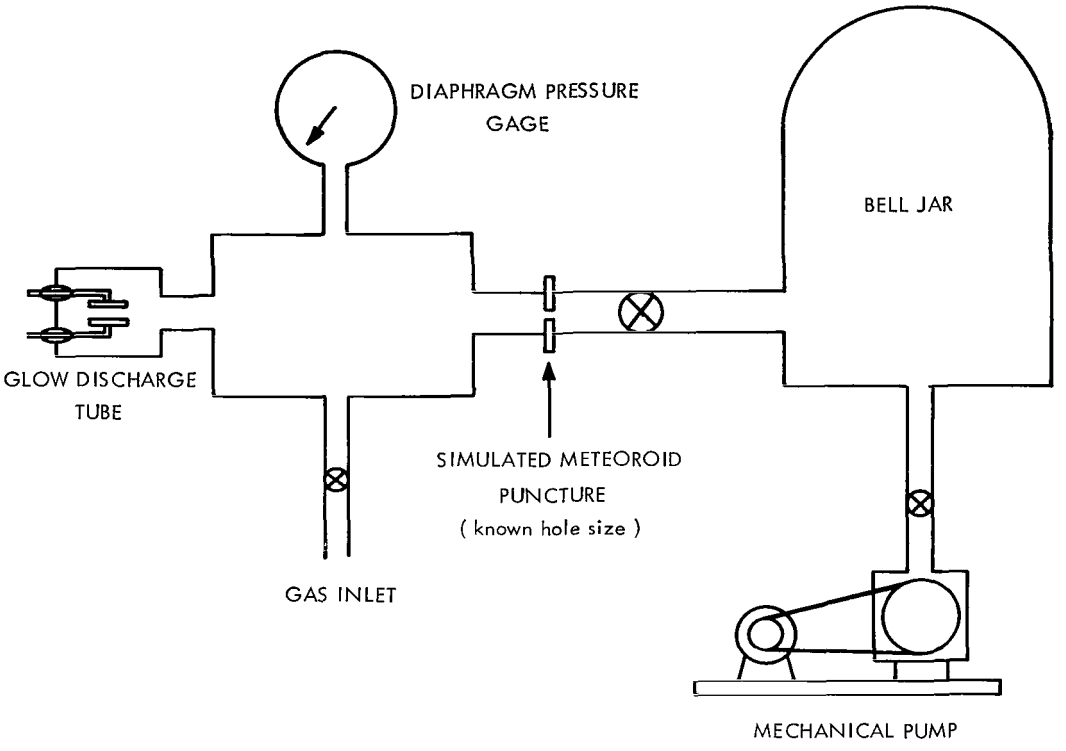

Figure 4.- Diagram of test chamber and vacuum system.

185 cm^3, chosen to approximate the volume of existing detector cells, and an O-ring coupling for ease in attaching the experimental gages. The pressure within the chamber was monitored by a strain-gage pressure transducer having a calibrated range of 0 to 20.7 kN/m^2 and a diaphragm gage with a range of 0 to 107 kN/m^2. To control the pressure, the test chamber was connected to a vacuum system consisting of a mechanical pump and a 0.11-m^3 bell jar, which served as a ballast tank while the test gas was introduced into the chamber through a desiccant and a metering valve.

To study the dependence of the glow discharge tube on leak rate, several 0.05-mm-thick stainless-steel disks, punched with holes varying in diameter from 0.025 to 1 mm, were placed in the tubing connecting the test chamber with the vacuum system. The

connecting tubing and valve were chosen so that their conductance would be much larger than that of any of the punched disks used.

The dc voltage required for the operation of the discharge tube was supplied by a variable (0 to 555-volt), highly regulated, power supply with a maximum load current of 300 mA. This power supply was monitored by a digital voltmeter with an input impedance of 10 MΩ. The discharge current was measured by observing the voltage drop across a 10-kΩ resistor in series with the experimental model. (See fig. 5.) This voltage was observed with a strip-chart recorder having an input impedance of 1 MΩ and 14 measurement ranges from 25 mV full scale to 500 volts full scale.

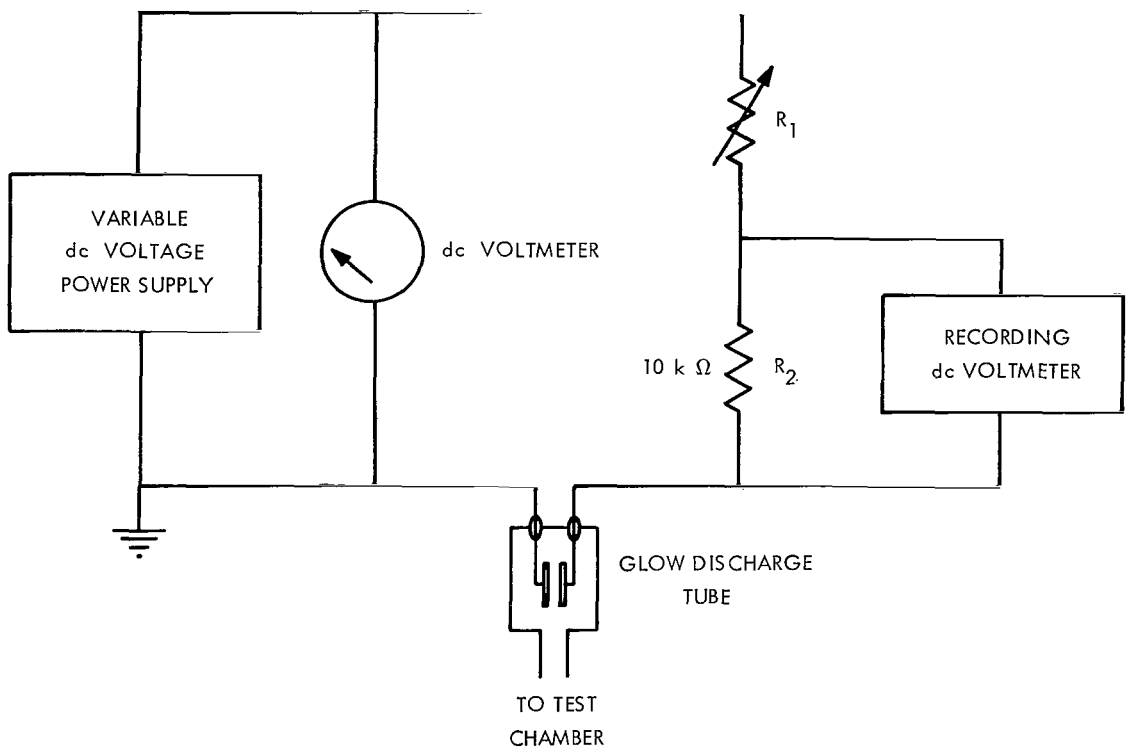

Figure 5.- Test circuit for determining the dc voltage characteristics of glow discharge tubes.

In attempting to optimize the configuration of the discharge tube and operating parameters for the specific purpose of this experiment, four different electrode geometries were tested. (See fig. 6 and table 1.) These different configurations were made by using ceramic-to-metal feed-throughs soldered into a 1.1-cm-diameter copper tube, 1.5 cm in length, which was attached to the test chamber.

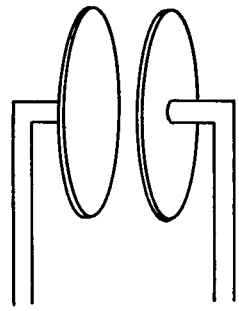

(a) Parallel disks.

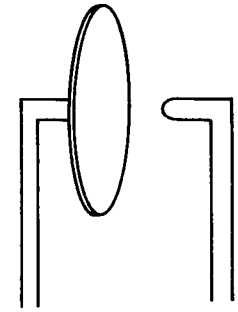

(b) Point and disk.

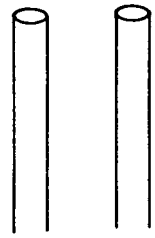

(c) Parallel wires.

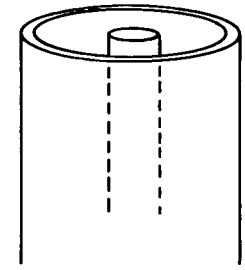

(d) Wire and coaxial cylinder.

Figure 6.- Electrode geometries.

EXPERIMENTAL PROCEDURE

A cursory study of the theory of electrical breakdown in gases revealed that the breakdown mechanism is dependent on the geometry of the discharge tube, the electrode material, the applied voltage, and the ionizing gas. To simplify the investigation, the dependence on two of these parameters, the ionizing gas and the electrode material, was eliminated. Helium was chosen as the ionizing gas because (a) its small molecular size would produce less impedance in flowing through the small orifices created by micrometeoroid punctures, (b) its low boiling point would permit its use for deep-space probes by reducing the possibility of its liquefying and altering the performance of the sensor, (c) it is the most common tracer gas used for leak detection and hence would simplify reliability testing of the resulting flight sensors, and (d) its low minimum breakdown potential would result in reduced voltage and power requirement for any flight instrumentation. In addition, the dependence of the breakdown mechanism on electrode material was ignored because the electrode surface had an absorbed gas layer that would be virtually the same for all materials unless it was removed by extensive cleaning and degassing. Experimental tests were then performed by varying the remaining parameters to obtain a discharge tube with suitable operating characteristics.

A preliminary model was constructed with flat, parallel disk electrodes (fig. 6(a)) and mounted in the vacuum system. The total resistance R_1 and R_2 in series with the glow discharge tube (fig. 5) was varied to determine its influence on the discharge characteristics. At a constant pressure in the conduction region $\left(p_o = 6.35\ kN/m^2\right)$ the applied voltage V_a was increased until breakdown occurred. While the voltage drop across R_2 was observed, R_1 was varied from zero to 9.99 MΩ. As the resistance was increased, the voltage drop across the discharge tube $V_r = V_a - i\left(R_1 + R_2\right)$ decreased to a value that would not sustain the discharge. Once quenched, the voltage drop across the discharge tube built back up to a level that again caused it to breakdown. This caused the current in the circuit to oscillate at a frequency dependent upon the time constant of the inherent resistance-capacitance circuit with the discharge tube behaving like a capacitor. This phenomenon was observed at all resistances greater than 0.5 MΩ (table 2 and fig. 7). To eliminate these oscillations and still maintain low power consumption in the circuit, all further tests were conducted by using a total resistance of 0.1 MΩ in series with the discharge tube.

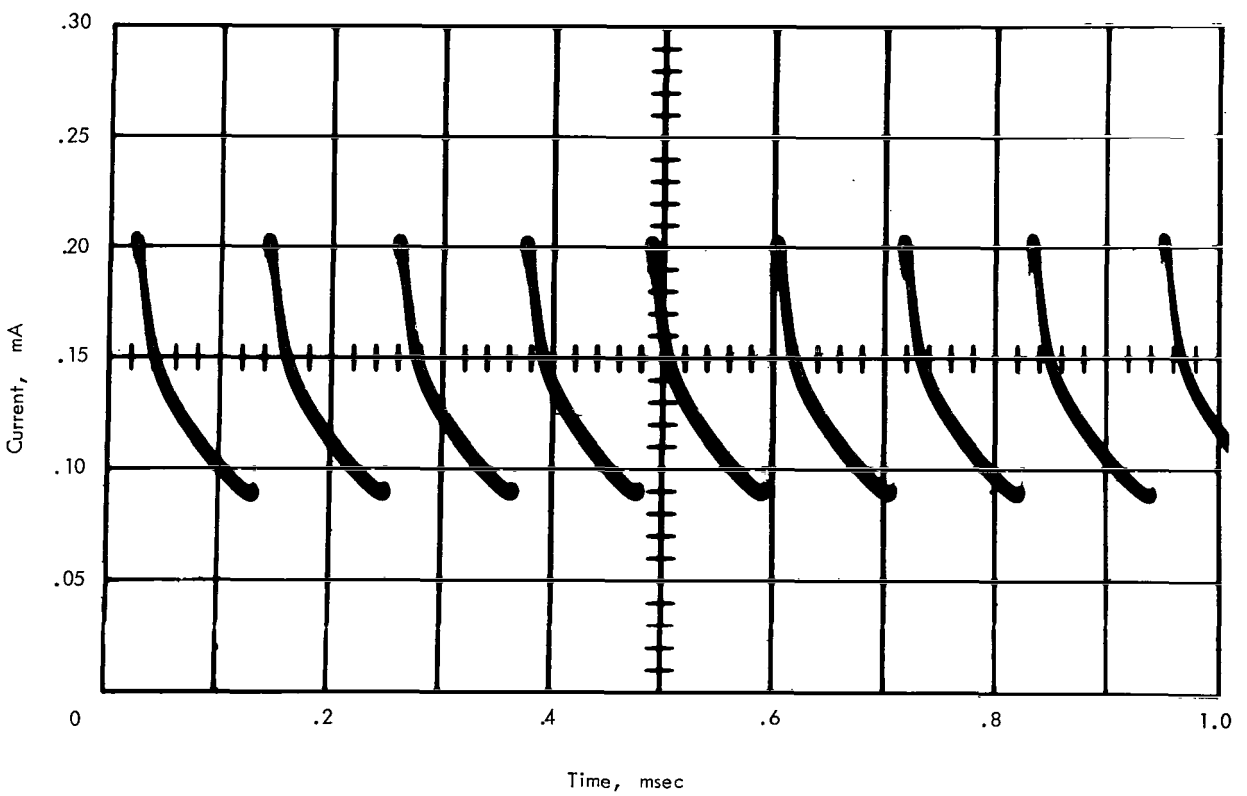

Figure 7.- Current oscillations for glow discharge between flat, parallel disks with external resistance of 1.0 MΩ. (See table 2.)

Paschen curves were generated for five different experimental models, two of which had identical electrode geometries but reversed polarity. (See figs. 8 to 12.) These data were obtained by holding the pressure constant within the discharge at some given value and increasing the applied voltage in 5-volt steps until breakdown occurred. The gaseous discharge was investigated throughout the pressure range from 0.207 to 107 kN/m^2 at 25° C, and the voltage was increased at 1-minute intervals to eliminate the possibility of some transient phenomenon, or lack thereof, preventing the breakdown from occurring. (Initiatory electrons leading to the breakdown of the gas are generated typically by external agents such as cosmic rays, and their appearance is thereby subject to the statistical fluctuations associated with that phenomenon.)

The criterion used for determining the optimum electrode configuration was the lowest minimum breakdown potential observed in a comparison of the Paschen curves. For simplicity, the data shown in figures 8 to 12 were subjected to a second-order least-squares fit, and the resulting equations differentiated to determine both the minimum breakdown potential and the pressure at which that breakdown would occur (table 3).

The geometry chosen was the wire cathode and coaxial cylinder anode with the wire grounded. The minimum breakdown potential for this configuration is 300 volts and occurs at a reduced gas pressure of 7.1 kN/m^2. All subsequent data are referenced to this model (fig. 13). In order to use this discharge tube with a pressurized cell to detect meteoroid punctures, two operating parameters had to be selected, the applied voltage and the initial pressure within the cell and connecting sensor. The operating voltage was chosen to be 350 volts, 50 volts greater than the minimum breakdown potential, to insure that the discharge tube would break down. From the Paschen curve for this model (fig. 12), an applied voltage of 350 volts should cause the discharge tube to break down at the reduced gas pressure of 3.3×10^4 N/m^2. The initial pressure in the detector, therefore, was selected approximately 100 percent greater (6.7×10^4 N/m^2) to guarantee that under reasonable temperature ranges, the discharge tube would not break down before a puncture occurred. The usefulness of the discharge tube to detect meteoroid punctures and determine the size of puncture was tested by observing the time rate of change of discharge current as the pressure within the detector cell decreased through the conduction range for a variety of simulated punctures.

The test chamber was first flushed with helium and then pressurized to 73.3 kN/m^2 at 25° C. The voltage was applied to the sensor and held for 5 minutes to observe any premature discharge. The test chamber was then pumped out at a rate dependent on an orifice in the vacuum line (fig. 4) simulating a meteoroid puncture. As the pressure within the detector decreased, the breakdown was recorded by the voltage drop across R_2 (fig. 5). The time rate of change of the discharge current was calculated from this voltage pulse. A typical example of this discharge pulse is shown in figure 14.

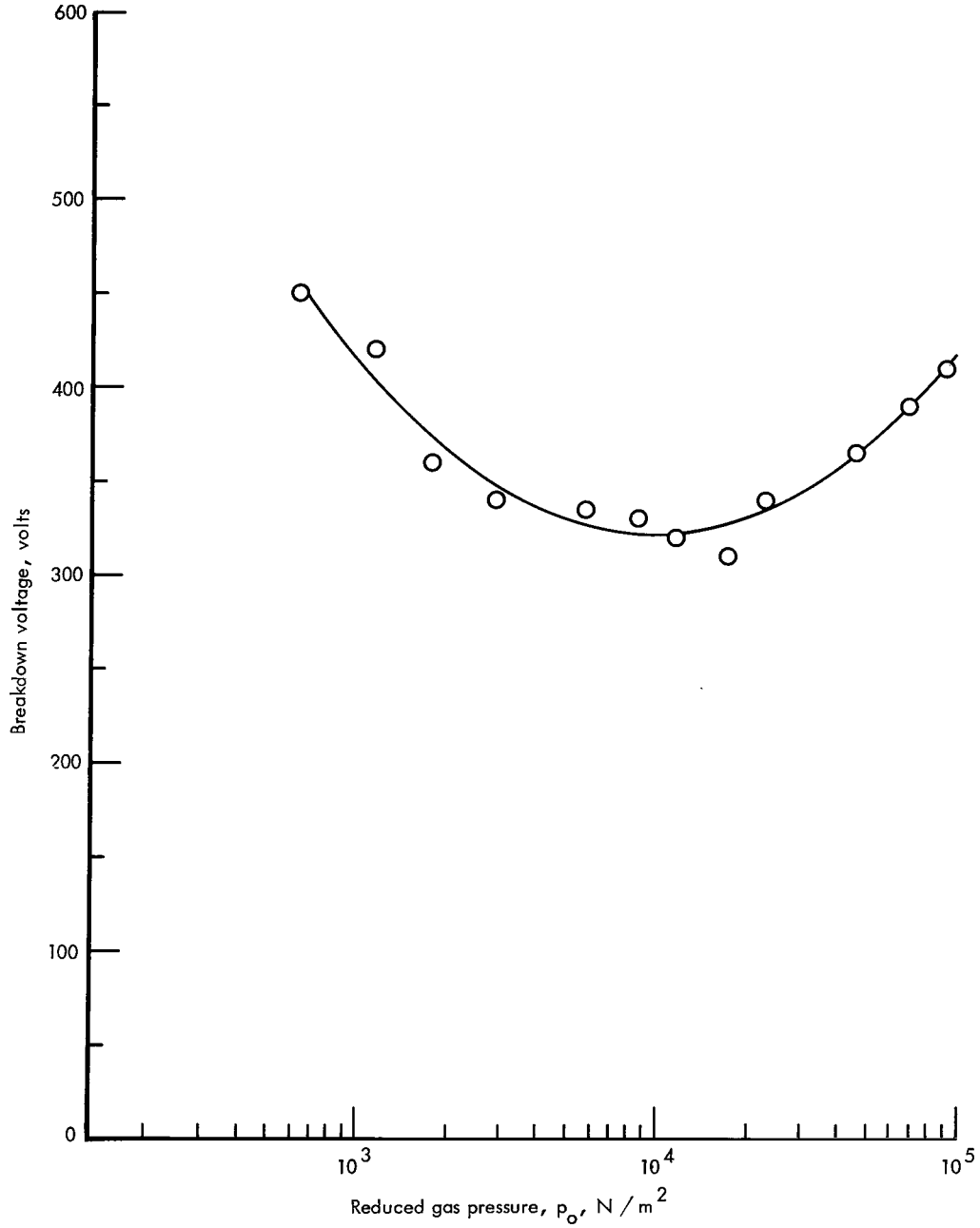

Figure 8.- Breakdown voltage between flat, parallel disks as a function of reduced gas pressure.

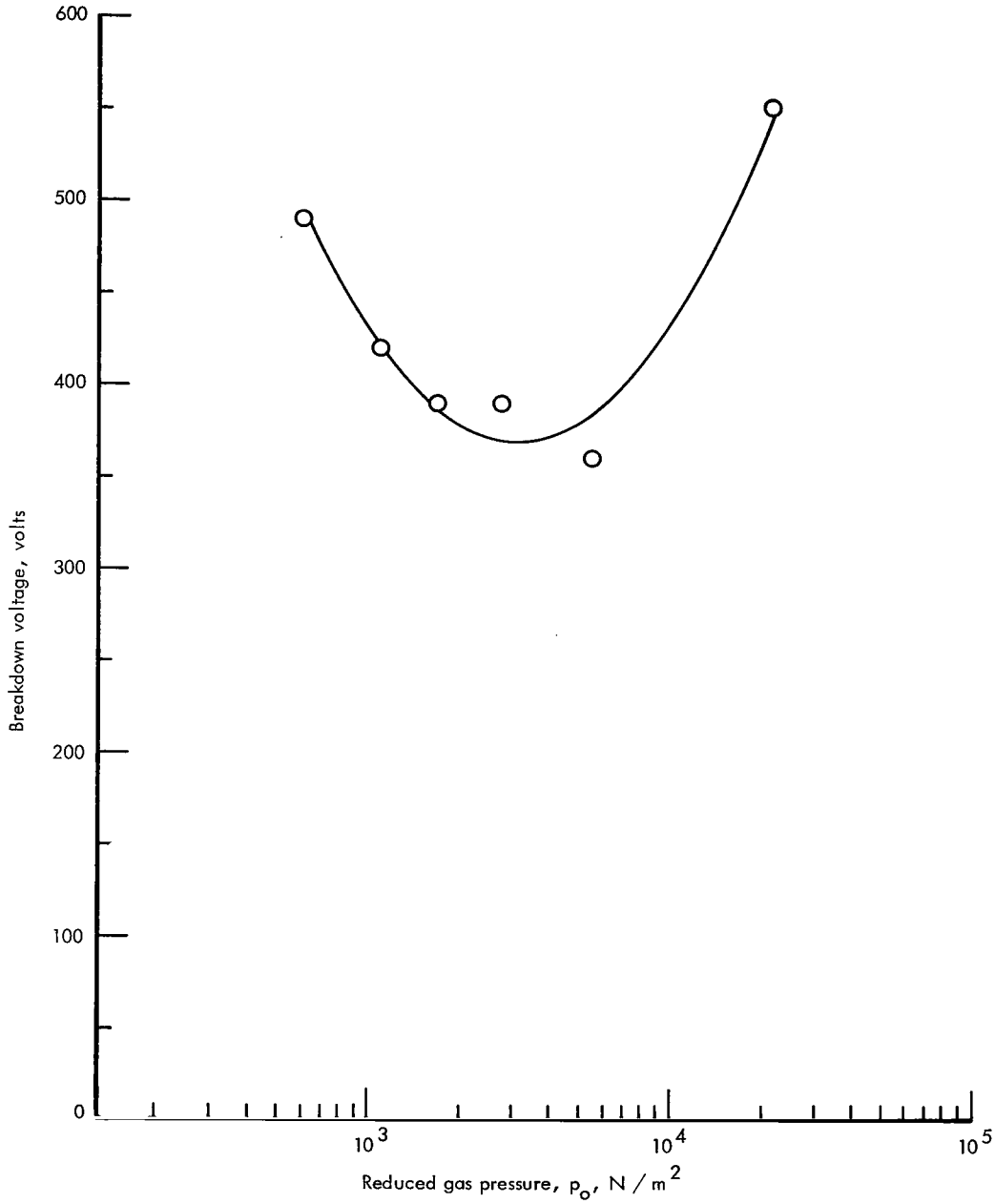

Figure 9.- Breakdown voltage between point anode and flat-disk cathode as a function of reduced gas pressure.

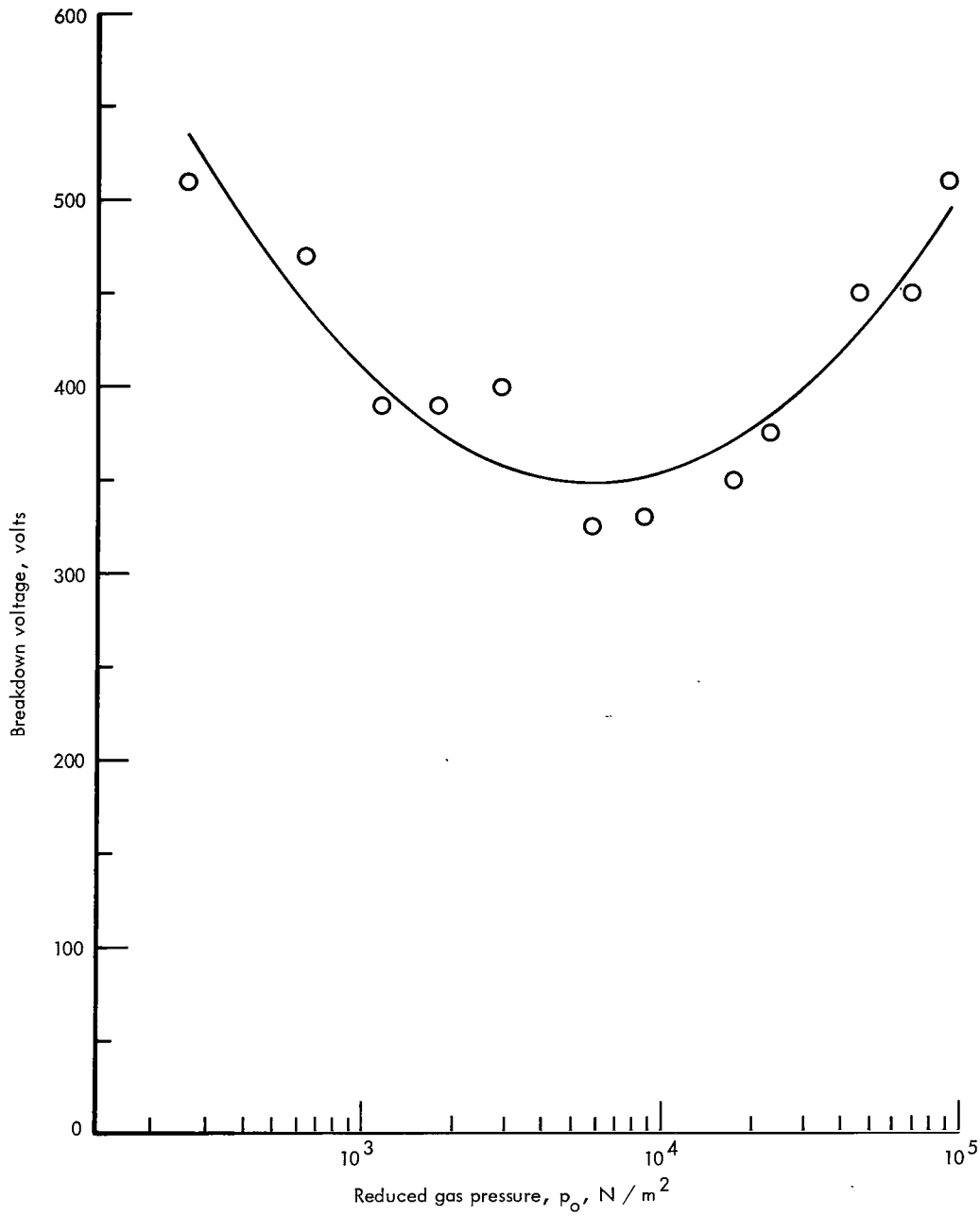

Figure 10.- Breakdown voltage between parallel wires as a function of reduced gas pressure.

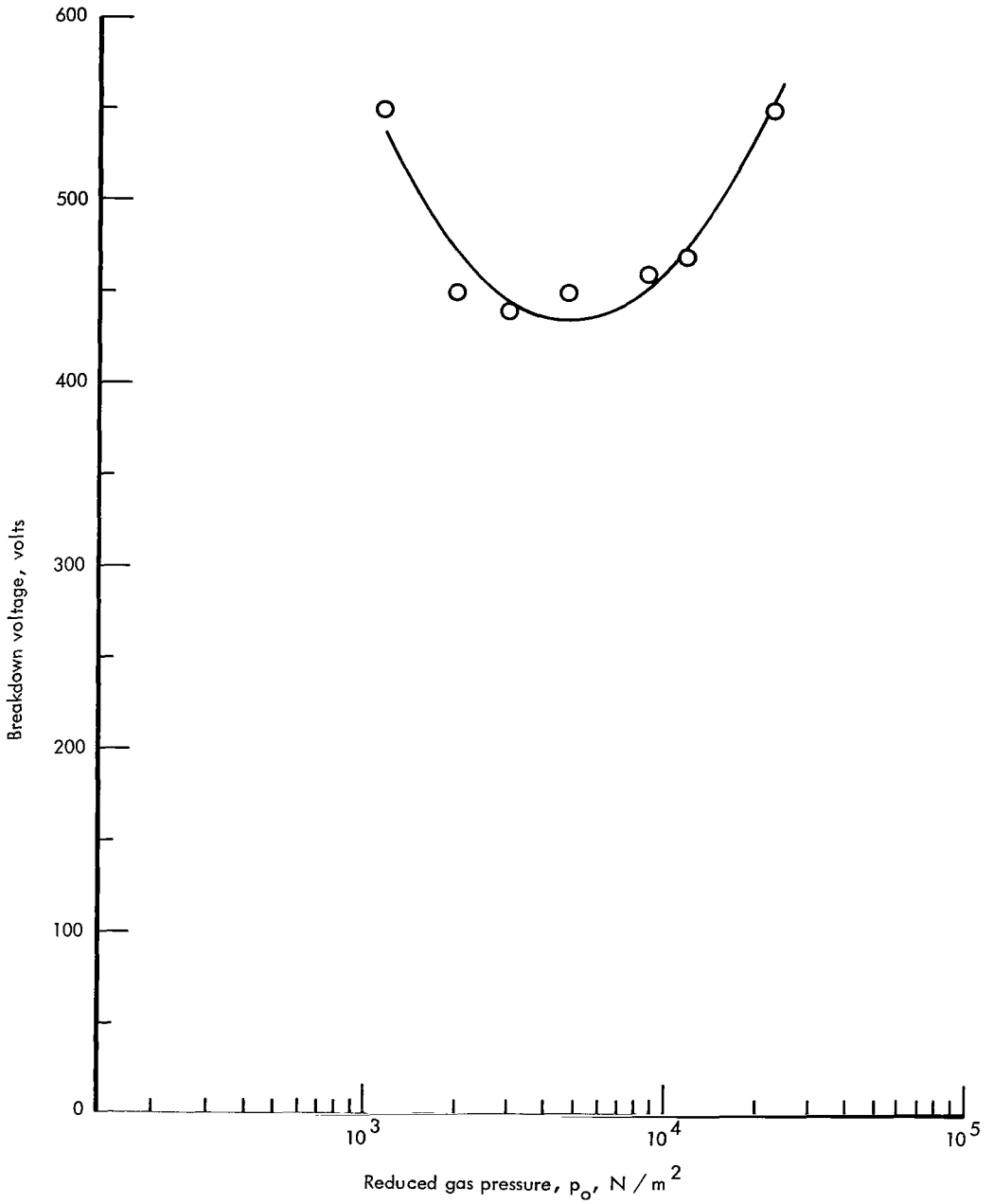

Figure 11.- Breakdown voltage between wire anode and coaxial cylinder cathode as a function of reduced gas pressure.

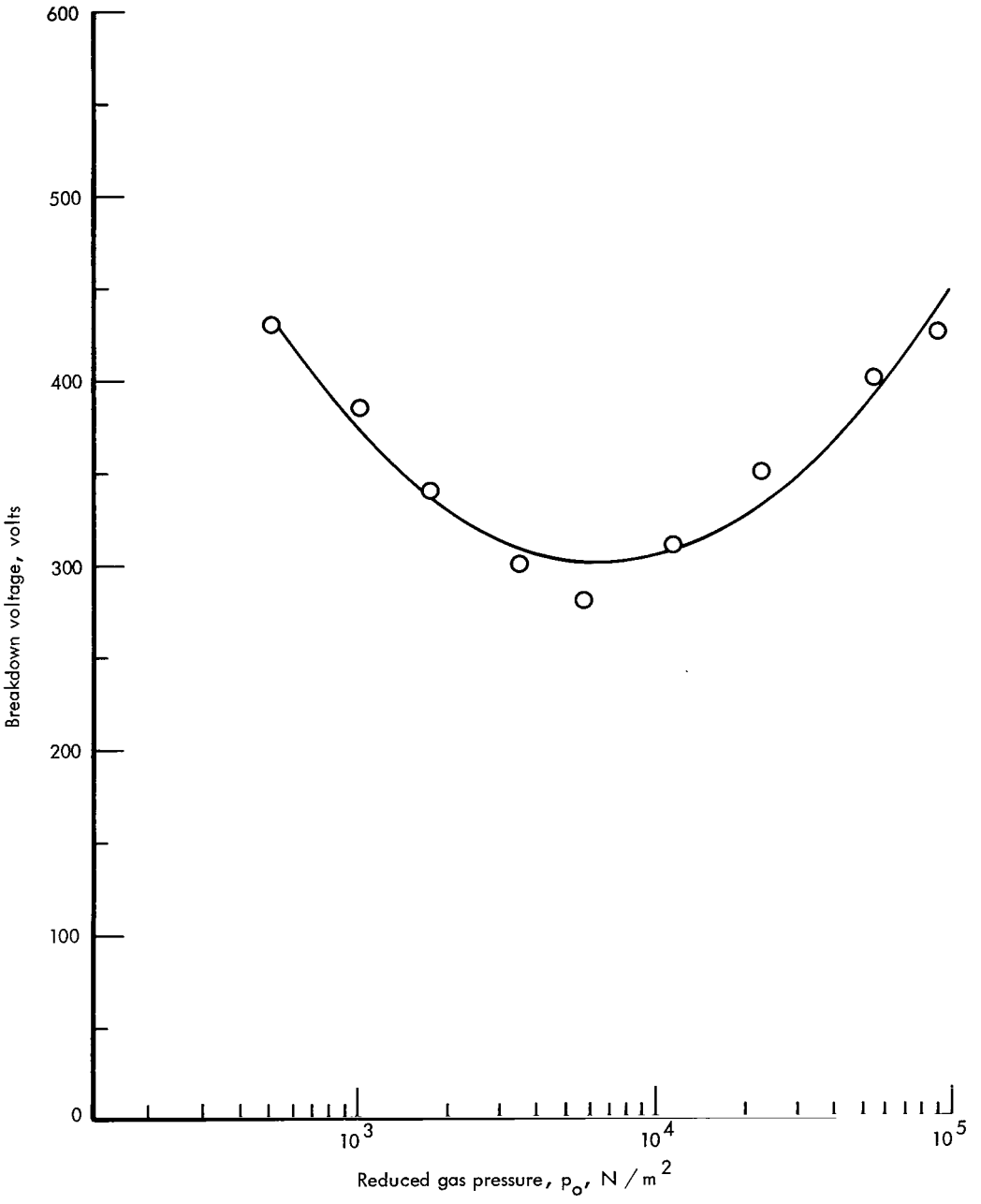

Figure 12.- Breakdown voltage between wire cathode and coaxial cylinder anode as a function of reduced gas pressure.

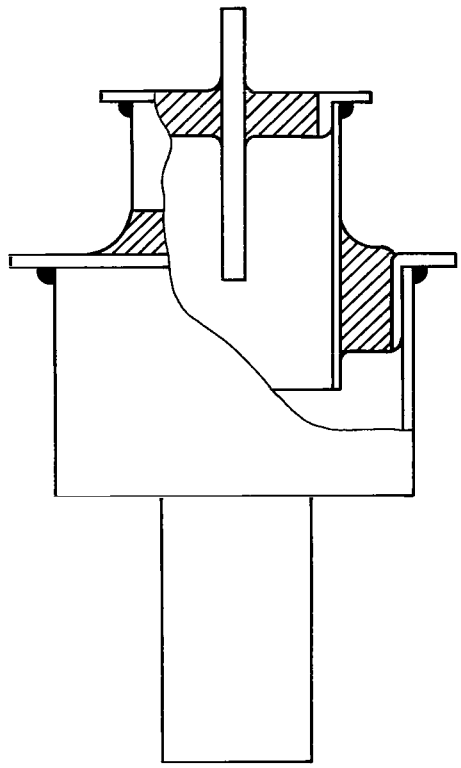

Figure 13.- Discharge tube (wire and coaxial cylinder electrodes) used to investigate determination of meteoroid puncture size.

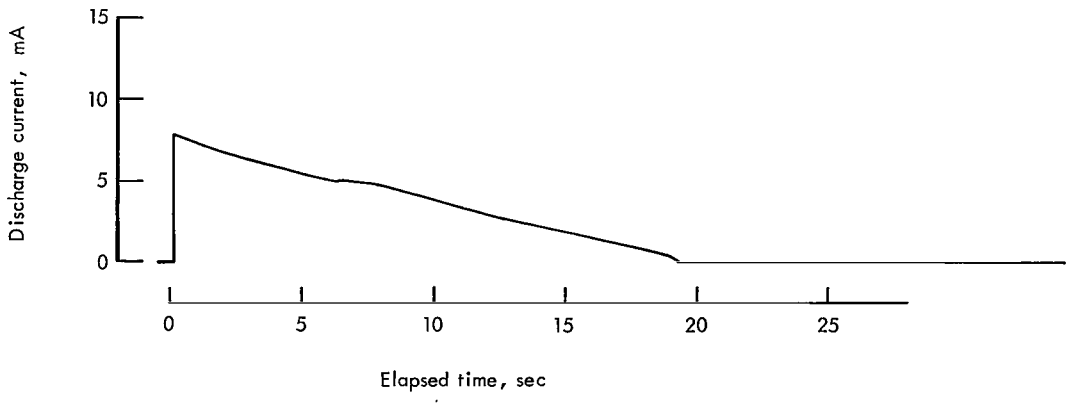

Figure 14.- Discharge pulse for 0.25-mm-diameter orifice. V_a = 350 volts.

DISCUSSION OF RESULTS

The discharge pulse shown in figure 14 is characteristic of the current flowing through the experimental gage during a simulated meteoroid puncture; that is, the current after the discharge had been initiated decreased linearly with time even though the pressure within the detector cell decayed exponentially. In varying the size of the simulated meteoroid puncture, both the period of the discharge pulse and the rate di/dt at which the discharge current decreased seemed to be functions of the resulting change in pressure decay. Closer inspection showed that the period of the discharge pulse for any given puncture size varied by as much as 100 percent of the lowest value, whereas the time rate of change of discharge current was repeatable once the discharge had been initiated.

An analysis of the gas flow through an orifice and the observed linear dependence of the discharge current on time (appendix A) suggested that di/dt should be proportional to the area of the orifice, that is, the size or area of a meteoroid puncture could be easily determined by measuring the time rate of change of discharge current during the pressure decay in a detector cell. Two discharge tubes were calibrated and the area of the simulated meteoroid punctures plotted as a function of di/dt. It was observed that as the area of the orifice became very small, di/dt seemed to be approaching some minimum value. The data were therefore subjected to a first-order least-squares fit, and the results show that it is indeed a better fit than would be obtained by assuming a simple proportionality relationship. Figure 15 shows a log-log plot and the linear fit of the data. The resulting first-order equations are of the form

$$A = a_0 + a_1 \frac{di}{dt}$$

where a_0 would represent a lower limit on the size of meteoroid puncture detectable by the discharge tube. The deviation of the data from the expected direct proportionality relationship is probably due to the gas flow through the smaller orifices being in the transitional and molecular regime rather than in viscous flow, as assumed in appendix A.

The error involved in using the linear equations to determine the area from a measured di/dt was calculated (appendix B) and the resulting fractional error plotted against the calculated area from the fitted curve (fig. 16). It can be seen in figure 16 that for an orifice area larger than 2.5×10^{-8} m^2 the error is less than 20 percent. For smaller holes, the error becomes too large for this method to be much more than a rough indication of the hole size. Even at best, the data show that for holes smaller than 10^{-9} m^2 the method becomes impractical.

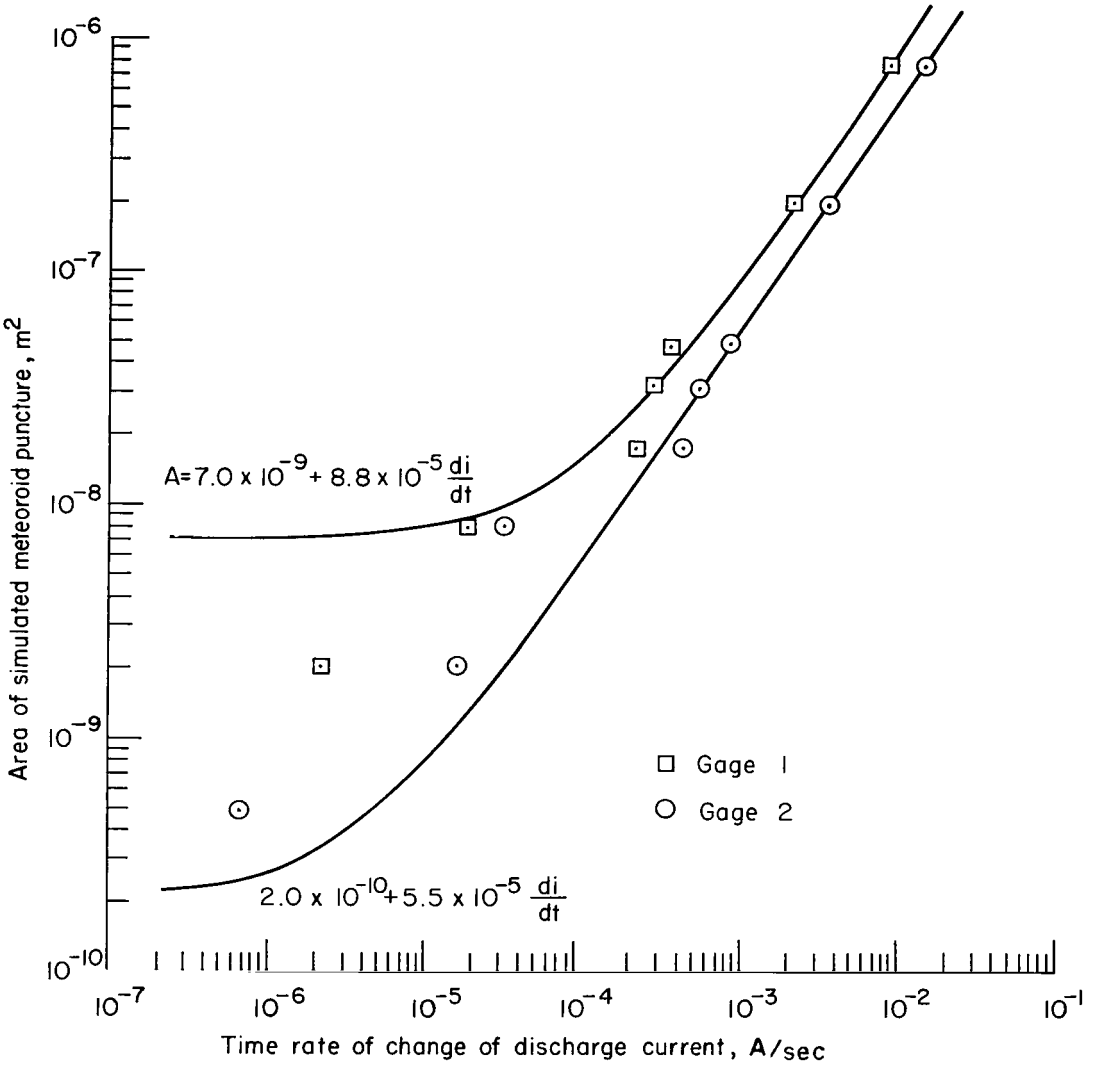

Figure 15.- Calibration of experimental gages.

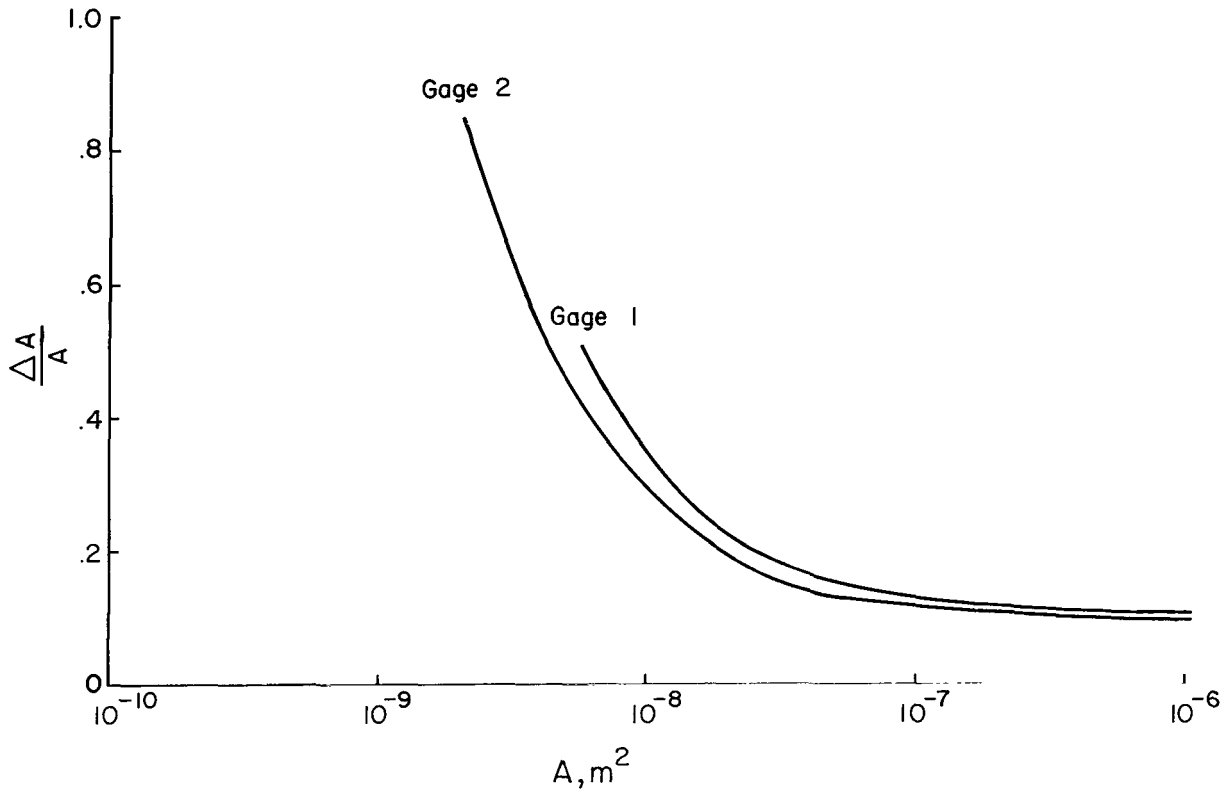

Figure 16.- Fractional error arising from use of calibration curves.

CONCLUSIONS

A study was conducted on the feasibility of using a cold-cathode glow discharge tube to observe the meteoroid puncture of pressurized detectors. This was accomplished by determining the optimum design characteristics for the discharge tube and then testing its operation by simulating meteoroid punctures with orifices ranging in diameter from 0.025 to 1 mm. The following conclusions were drawn from this investigation:

1. The cursory studies showed that a cold-cathode glow discharge tube could be used with existing pressurized meteoroid detector cells and would weigh 80 times less than the pressure sensors currently used (0.9 g compared with 78 g).

2. The optimum electrode geometry for such a discharge tube was a thin wire cathode and coaxial cylinder anode with the wire grounded.

3. The characteristics of the discharge pulse obtained in detecting a meteoroid puncture can be used to determine the approximate size of the hole created by the meteoroid and thereby an estimate of the size of the meteoroid itself.

Additional study is necessary to learn if there are any adverse effects on the operation of the discharge tube caused by the environment of space, for example, large temperature variations, solar and galactic particle radiation, and electromagnetic interference. Investigation of the effects of gas composition and electrode material on the discharge might extend the sensor range for determining the meteoroid puncture size.

Langley Research Center,
National Aeronautics and Space Administration,
Hampton, Va., July 27, 1971.

APPENDIX A

DERIVATION OF THE di/dt DEPENDENCE ON ORIFICE SIZE

According to the equation of state,

$$pV = NkT$$

a given quantity of gas can be defined by the product of its pressure and volume at a given temperature. The rate of change of the quantity of gas is therefore

$$p\frac{dV}{dt} + V\frac{dp}{dt}$$

or merely

$$V\frac{dp}{dt}$$

for a constant volume.

In viscous flow where the mean free path is small compared with the dimensions of the orifice, the flow depends on the ratio of low pressure to high pressure $r = p_2/p_1$ and the ratio of the specific heats of the gas γ. The gas flow is thus given by the following equation adapted from Prandtl (ref. 6, pp. 16-17):

$$Q = \left[\frac{2\gamma kT}{M(\gamma - 1)}\right]^{1/2} r^{1/\gamma}\left[1 - r^{(\gamma-1)/\gamma}\right]^{1/2} p_1 A$$

At low pressure ratios $p_1 > 10p_2$, the gas streams with the velocity of sound, and the flow is independent of p_2, that is,

$$Q = KpA$$

where K is the proportionality constant under the conditions of reduced pressure and temperature produced by the adiabatic expansion through the orifice. Since the rate of change of the quantity of gas in a system must equal the gas flow rate into a system $(+Q)$ or the flow rate out $(-Q)$,

$$V\frac{dp}{dt} = -KpA \tag{A1}$$

for a system losing gas. Integrating equation (A1) and setting $p = p_i$ at $t = 0$ yields

$$p = p_i e^{-KAt/V} \tag{A2}$$

Empirically the discharge current i is observed to vary linearly with $\ln p$, independent of the rate at which the pressure decays (fig. 17), that is,

$$i = a + b \ln p \tag{A3}$$

Substituting equation (A2) into (A3) gives

$$i = a + b\left(\ln p_i - \frac{KA}{V} t\right) \tag{A4}$$

Taking the first derivative with respect to time of equation (A4) yields

$$\frac{di}{dt} = -\left(\frac{bK}{V}\right)A$$

which indicates that di/dt should be proportional to the area or size of the orifice.

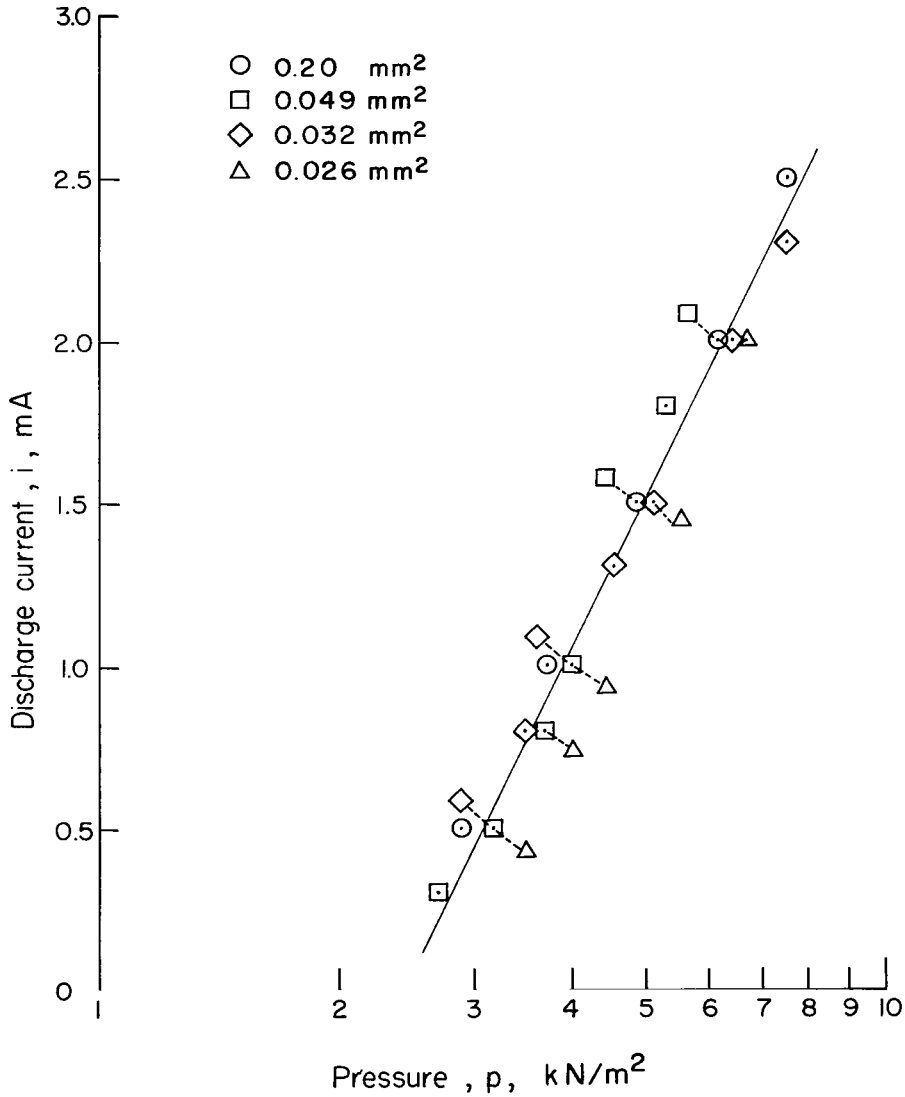

Figure 17.- Discharge current as a function of pressure for different rates of pressure decay depending on area of pumping orifice.

APPENDIX B

UNCERTAINTY IN USE OF LINEAR CALIBRATION CURVES

A calculation of the uncertainty involved in using the calibration curves to determine the orifice area from a measured di/dt can be made from the uncertainty in fitting the data to a first-order equation

$$A = a_o + a_1 \frac{di}{dt}$$

considering the variation in each quantity

$$A + \Delta A = a_o + \Delta a_o + \left(a_1 + \Delta a_1\right)\left(\frac{di}{dt} + \Delta \frac{di}{dt}\right)$$

or

$$A + \Delta A = a_o + a_1 \frac{di}{dt} + \Delta a_o + \Delta a_1 \frac{di}{dt} + a_1 \Delta \frac{di}{dt} + \Delta \frac{di}{dt} \Delta a_1$$

Subtracting A from both sides of the equation and neglecting the products of the variations yields the desired variation in area,

$$\Delta A = \Delta a_o + \Delta a_1 \frac{di}{dt} + a_1 \Delta \frac{di}{dt}$$

The variations in the constants a_o and a_1 were determined from the root mean square of the area deviations about the fitted linear equation (ref. 7) (table 4), whereas the variation in di/dt was estimated to be within 10 percent of the graphically determined value based on the maximum and minimum slope observed in any given discharge pulse. Figure 16 shows a plot of the fractional error $\Delta A/A$ as a function of the computed area for the calibration curves of both experimental gages.

REFERENCES

1. Neswald, Ronald G.: The Meteoroid Hazard. Space/Aeronaut., vol. 45, no. 5, May 1966, pp. 76-85.

2. Acton, J. R.; and Swift, J. D.: Cold Cathode Discharge Tubes. Academic Press, Inc., 1963.

3. Llewellyn-Jones, F.: Ionization and Breakdown in Gases. John Wiley & Sons, Inc., c.1957.

4. Morgan, C. Grey: Fundamentals of Electric Discharges in Gases. Handbook of Vacuum Physics, Vol. 2, Pt. 1, A. H. Beck, ed., Pergamon Press, Inc., c.1965.

5. Wollan, D. S.; Trower, W. P.; Ramamurti, K.; and Meshejian, W. K.: Gas Density Detector for Use in Space. Contract No. NAS 1-8145, Virginia Polytech. Inst., Oct. 1969. (Available as NASA CR-66834.)

6. Guthrie, A.; and Wakerling, R. K., eds.: Vacuum Equipment and Techniques. McGraw-Hill Book Co., Inc., 1949.

7. Topping, J.: Errors of Observation and Their Treatment. Third ed., Chapman & Hall, Ltd., 1962.

TABLE 1.- EXPERIMENTAL ELECTRODE GEOMETRIES

[Electrode separation was 1 mm]

Anode		Cathode	
Material	Geometry	Material	Geometry
304 stainless steel	Disk, 3-mm radius	304 stainless steel	Disk, 3-mm radius
Nichrome	Hemisphere, 0.5-mm radius	304 stainless steel	Disk, 3-mm radius
Nichrome	Wire, 1.0-mm diameter, 4.5-mm length	Nichrome	Wire, 1.0-mm diameter, 4.5-mm length
Kovar	Wire, 0.8-mm diameter, 4.0-mm length	Kovar	Cylinder, 2.7-mm inside diameter, 7.0-mm length
Kovar	Cylinder, 2.7-mm inside diameter, 7.0-mm length	Kovar	Wire, 0.8-mm diameter, 4.0-mm length

TABLE 2.- CHARACTERISTICS OF THE GLOW DISCHARGE BETWEEN FLAT, PARALLEL DISKS

$[V_a = 250$ volts; $p_o = 6.35$ kN/m$^2]$

External resistance, $R_1 + R_2$, MΩ	Conditions at breakdown		Conditions after breakdown		Frequency, kHz
	i_{min}, mA	$V_r = V_a - i_{min}R$, V	i_{max}, mA	$V_r = V_a - i_{max}R$, V	
0.10	0.80	170	0.80	170	----
0.20	0.45	160	0.45	160	----
0.50	0.18	160	0.23	135	22
[a]1.0	0.06	190	0.17	80	8.3
10	0.006	190	0.017	80	1.2

[a]See figure 7.

TABLE 3.- MINIMUM BREAKDOWN POTENTIAL FOR VARIOUS ELECTRODE GEOMETRIES IN HELIUM

Electrode geometry	Minimum breakdown potential, $V_{s,min}$, V	Reduced gas pressure, p_o, at $V_{s,min}$, kN/m^2
Flat, parallel disks	320	10
Disk cathode and point anode	370	3.5
Parallel wires	350	6.1
Wire anode and coaxial cylinder cathode	435	5.1
Wire cathode and coaxial cylinder anode	300	7.1

TABLE 4.- COEFFICIENTS AND THEIR STANDARD ERRORS FOR A LEAST-SQUARES FIT OF THE DATA TO LINEAR EQUATION $A = a_0 + a_1 \frac{di}{dt}$

Gage	a_0, m^2	Δa_0, m^2	a_1, m^2-sec/A	Δa_1, m^2-sec/A	Correlation coefficient
1	7.0×10^{-9}	3.1×10^{-9}	8.8×10^{-5}	8.9×10^{-7}	0.99975
2	2.0×10^{-10}	1.5×10^{-9}	5.5×10^{-5}	2.8×10^{-7}	0.99993

NASA-Langley, 1971 —— 14 L-7794